Mathematics and Systems Science 2025, 3(3), 3384.
https://doi.org/10.54517/mss3384

Article

Parallelism, traveling waves and modular biodiversity interfaces in non-stationary ecosystems

Wilfried Allaerts

Biological Publishing A&O and Immunology Department, Erasmus University Medical Center, 3015 GD Rotterdam, Netherlands; w.allaerts@planet.nl

CITATION

Allaerts W. Parallelism, traveling waves and modular biodiversity interfaces in non-stationary ecosystems. Mathematics and Systems Science. 2025; 3(3): 3384. https://doi.org/10.54517/mss3384

ARTICLE INFO

Received: 5 March 2025
Revised: 16 June 2025
Accepted: 18 June 2025
Available online: 12 August 2025

Abstract: The present paper treats mainly two questions, namely the mathematical characterization of the notion of biodiversity of a border interface between two adjacent ecosystems, and the role of human interference in the physical reality of interacting multi-species systems. Mathematically, the techniques of reaction-diffusion modeling, Turing's notion of flow matrices and Verhulst logistic growth dynamics are introduced, in order to model the complex interactions in a fractal, non-stationary ecosystem. A new key approach is the combined use of flow matrices and Verhulst growth dynamics with Laplace transforms. However, these findings so far remain theoretical, not in the least because of the widespread interference of human activities with ecological developments, both planned and unplanned. When comparing mathematical models and the actual physical dynamics of ecosystems, parallel trends as well as species-specific, unique deviations are conspicuous. Especially the latter remain hard to predict, indicating the limited value of mathematical predictions for the actual biodiversity trends in the field. Moreover, in a specific case study from the Netherlands related to the ecology of game mammals and a top-predator (the Wolf), it appears that not only contemporary ecological management operations, but also the contingency of measures from a historical past (exceeding 200 years) play a significant role in understanding the human interference factor in nature (designated as the Anthropocene factor).

Keywords: biodiversity of border interface; reaction-diffusion modeling; Turing's flow matrices; Verhulst logistic growth; multi-species ecosystems; history of Raven-Wolf-Deer alliance

1. Introduction

In contemporary ecological monitoring, the almost simultaneous occurrence of waves of extinction, disease epidemics and other ecological disasters is often recognized. Sometimes, a common cause has been pinpointed, such as environmental pollution through pesticides [1], oceanic heat waves [2], or pandemics like avian influenza causing the sudden death of thousands of Puffins, Razorbills and Guillemots [3]. In other cases, it is more difficult to indicate a common cause, although a strikingly parallel development may have been found. Take for instance the rise of bovine tuberculosis (TBC) in British cattle [4] and the Bluetongue epidemic in cattle and sheep (and in wild ruminants too) in Continental Europe in the last decade, and the disappearance of flowering herbs and (pollinating) insects in grasslands [5]. Recently, since January 2025, also Foot- and Mouth disease (FMD) was detected in Water Buffalos (*Bubalis bubalis*) in Germany, but, fortunately, so far, the latter epidemic didn't spread to the Netherlands.

Parallel developments may often appear, without having a clear relationship: they may represent unrelated coincidences, or, a hidden variable may be present that we still have to unveil. For instance, the sudden (migratory) invasion of thousands of millions of one species of dragonflies, the Common Darter (*Sympetrum striolatum*) in North-Western Europe in the last week of August 2024, and the elevated numbers of a particular Finch species, the Greenfinch (*Carduelis chloris*). The Greenfinch, however, is not known as a migrating bird species. Also, it is known as an herbivorous species, predominantly feeding on seeds and only occasionally (in the cold winter months) it may supplement its diet with small insects. So, the coincidence of the peak density numbers of both species, seems entirely fortuitous. Is it truly?

Since the eighties of last century, mathematicians have tried to capture and analyze the interspecies interactions in 2- and 3-species models as a modular system of ecosystem dynamics [6–10]. A common thread in these studies is the deterministic outset and modular approach, characterized by a limited number of well-defined variables (in a closed system), the condition of boundedness of the solutions and the finding of monotone, stable dynamical functions describing the ecosystem's behavior. This however may not very well correspond with common sense and direct observation in the present era of multiple climate problems and ecological catastrophes [11]. The occurrence of parallel developments may on the one hand suggest an abstract, perhaps mathematical invariant pattern; on the other hand, natural species may behave in a myriad of possibly different ways, whereby only a detailed analysis of the genetic, biochemical, behavioral, correlations between the species concerned may explain the interspecific interaction. Many examples of these exist in the kingdoms of insects, fungi, tree species, coral reef *Coelenterata*, fishes et cetera.

The pivotal question to be asked here is whether a different approach is possible, that meets the vigor of mathematical analysis and that moreover shows a better correspondence with the observed empirical observations? Although for the outcome of a single species birth-death process, both deterministic and stochastic approaches lead to the prediction of the same population size distribution [12], for the behavior of multi-species interaction systems it is more complex. Multi-species models may indeed show significant differences between the deterministic Volterra-like cycles [13] and cycles where stochastic noise effects are introduced, especially when also low abundancies occur for one or more species [12].

So far, most studies have also adopted a mean-field approximation of the population densities in their model. The biodiversity driving potential of borders between divergent habitats was recently introduced as a generator for biodiversity resilience [14]. In the present study, the premises and limitations of a non-stationary approach for ecosystem dynamics with a border (biodiversity) interface are outlined (see Section 2. Characteristic Features of an alternative approach for Non-Stationary Ecosystems). Then, the premises are worked out in a mathematical translation of the initial conditions (see Section 3. Mathematical characterization of the border interface and initial conditions). Moreover, attempts are presented to analyze the dispersion processes in a fractal border area, taking migration and interspecific interactions into consideration (Section 4. Parallel and anti-parallel developments). The mathematical techniques of flow matrices and Verhulst logistic growth dynamics appear to be very valuable in this respect. Doing so, the present ecosystem model may qualify as a non-linear dissipative structure, as suggested previously [15]. Finally, a field observation case, showing the importance of historical contingencies and species-specific idiosyncrasies are discussed (see Section 5. Historical contingencies and species-specific deviations).

2. Characteristic features of an alternative approach for non-stationary ecosystems

With due respect for the pioneers of mathematical ecology studies, we'd wish to state, in corroboration of the work of e.g., Law [16], that the esthetic qualities of the mathematical analysis and theoretical results so far have often outweighed the empirical corroboration of the underlying assumptions. Or, in other words, the beautiful symmetry of the mathematically constructed systems is (mostly) not reflected by the asymmetry of the actual, living world [17]. On the other hand, mathematical analyses that are not scientifically sound (whatever rules there are for defining what is sound and what isn't), or require unrealistic, imaginary fabrics without possible applications in the physical world, ultimately form a dead end too, for obvious reasons!

In the classical ecological models, dynamic equilibria are suggested to define the stable end stages of the ecosystems, quite analogous to chemical equilibria. And, also in analogy to chemical dynamic equilibrium reactions, the resulting concentrations of chemical substances remain constant, by definition. In mathematical ecology, these equilibrium situations are characterized by saddle points and local minima of the population densities. To infer from this analogy that also constant population densities result for the biological species involved in a 'stable' ecosystem, however, is not a flawless inference. Not only, because it is at variance with the observation of oscillating densities and seasonal migration and other sources of periodic fluctuations. There is also a more fundamental flaw in this comparison: in particular, the constant chemical concentrations at equilibrium (in a dynamic system) only refer to the chemicals that actually are in the (closed) environment where the equilibrium is established (and not for the chemical substances that are also involved in other chemical reactions, e.g., substances leaking out the compartment, etc., or interconnected equilibria). The latter is also true for so-called stable multiple-species ecosystems, making it more complicated to define stability of interactions when more than two (or three) species are involved [10].

A different approach is seen in the analysis of Law [16] and others, making use of the notion of (global asymptotic) Lyapunov stability in multi-species orbits [18–20]. One of the aims of the present study is to investigate whether this asymptotic Lyapunov stability can also be applied to the biodiversity of a multi-species border system between different ecological habitats, designated as the border interface.

Following the so-called 'persistence' approach, Law [16] developed criteria for coexistence of n species ('persistence' means that they are not dying out from the ecosystem), using a system of coupled ordinary differential equations (ODE) in an n-dimensional non-negative phase space. The criterion for coexistence of n species, according to common practice in theoretical ecology, is to evaluate the Jacobian matrix (J) in order to establish the existence of an equilibrium point $\hat{\mathbf{z}}$ with the property of asymptotic Lyapunov stability [18]. The test for asymptotic stability consists of evaluating the eigenvalues of J at the equilibrium point, of which the real parts should all be strictly negative [16]:

$$J = a_{ij} \text{ with } a_{ij} = \frac{\partial}{\partial x_i}\left(x_i \cdot f_i(x)\right)\Big|\, x = \hat{z}.$$

And, as it was also suggested by Law [16], the drawback that the asymptotic Lyapunov stability only applies for a small region around the equilibrium point, where the dynamic equations can be linearized, forward the problem of the linearization of the multi-species border system.

Multi-species orbits indeed may predict the cyclic and anti-cyclic fluctuations in abundance patterns of a number of co-habitant species. However, the geographical range dynamics, explaining the often local high abundance peaks of several (sometimes unrelated) species, whereas in other areas these very species are completely absent, or co-habit with totally different species, remain an unresolved problem [21]. This phenomenon has long been recognized for plant communities too. According to Hengeveld, the spatial dynamics of a species “result from its idiosyncratic physiology, anatomy and behavior, also expressed in, for instance, differences in seasonality, biotope preference, or in numerical build-up of its range” [21]. Nevertheless, also obvious parallel developments do occur, with an astonishing similarity in geographical preferences, like the high densities of herd-forming Red Deer (*Cervus elaphus*) and Wild Hogs (*Sus scrofa*) in the semi-enclosed territories of the High Veluwe National park of the Netherlands, and the exponential growth of the population of Wolves (*Canis lupus*) in that same area, with a yearly growing number of wolf packs since 2018 (so far, no full-scale wolf packs are observed outside that very area in the Netherlands) (see Section 5. Historical contingencies and species-specific deviations). We will come back to the notion of spatial range dynamics and to Hengeveld’s emphasis on “statistical geographic optimum-surface abundance distributions” as an opposite to the presupposed “simultaneous occurrence of equilibrium conditions” [21,22].

In order to translate these findings into a numerical modeling approach, therefore, many more variables have to be considered (for all possible inter-species interactions and not only a few selected species that are considered relevant), with the additional, complicating features that although species may be absent in a given area at some point, they may re-appear in another period (e.g., seasonal migrations). Or, they may pertain to the multi-species and multi-trophic ecosystem, although not present always and everywhere in the spatial range of their distribution. In a previous paper, we introduced the notion of time-integrated convolution of a fractal biodiversity function, as a means to combine the fractal appearance of spatial biodiversity patterns as well as the important concept of the border interface [14].

3. Mathematical characterization of the border interface and initial conditions

As an outset we suggest the mathematical characterization of the border interface to combine a boundary condition description adopted in analogy with Carslaw and Jaeger’s [23] solution for heat conduction in the semi-infinite solid with a defined flux (f) per unit time and unit area at $x = 0$, together with a discrete Poisson distribution in recursive form [24].

With a (constant) flux F_0 at $x = 0$ the differential equation is given by:

$$f = -K\frac{\partial v}{\partial x},$$

K being the thermal conductivity, which in reaction-diffusion theory represents the diffusion constant D. In the present case, we may think of an effective diffusion constant (D_{eff}) as a parameter related to the probability of a species (or an individual of this species) to enter the border interface.

The solution of the equation above, according to Carslaw and Jaeger [23] for $t > 0$, is:

$$f = F_0 erfc\frac{x}{2\sqrt{\kappa t}},$$

with F_0 representing the so-called dimensionless time (or Fourier number), allowing the combination of conductivity and time variables [25].

The resulting 'temperature' as a function of (x, t) then was found to be:

$$v = \frac{2F_0}{K}\sqrt{\frac{\kappa t}{\pi}}e^{-}\frac{x^2}{4\kappa t} - \frac{x}{2}erfc\frac{x}{2\sqrt{\kappa t}}.$$

In this case, the 'temperature' has to be replaced by the density of a certain species in the area for $x > 0$ and $t > 0$. However, we have to account for a community with multiple species, in order to speak of the biodiversity of an ecosystem (see Section 4.1). Also, the border interface may play an active role in generating the conditions for biodiversity resilience (see Section 4.3.). The diffusion process envisaged here, is rather comparable to the so-called time-fractional diffusion processes [26].

Moreover, the distribution of the different species not necessarily follows the same pattern for each species [24], also because species-specific characteristics like velocity of displacements (during migration, foraging or escaping from a predator), reproductive successes and niche dependencies are not easily described in a few formulas. Apart from the constant, uniform distribution case, the simplest form may be given by the Poisson distribution:

$$\frac{1}{e^{\mu}}, \frac{\mu}{1!e^{\mu}}, \frac{\mu^2}{2!e^{\mu}}, \frac{\mu^3}{3!e^{\mu}}, \dots \frac{\mu^r}{r!e^{\mu}},$$

which are the (discrete) successive counts of the rare event (Y). The expression above equals the terms of the infinite series expansion of e^{μ}, when each term is divided by e^{μ} (given that the parametric mean μ is known) [24]. In recursive form, it may be re-written as:

$$\widehat{f_i} = \widehat{f_{i-1}}\left(\bar{Y}/_{i}\right) \text{ for } i = 1, 2, 3, \dots \text{ where } \widehat{f_0} = e^{-\bar{Y}} = 1/_{e^{\bar{Y}}}.$$

In principle, the initial situation at $x = 0$ could be defined for each of the species (with sample means Y_i) entering the ecosystem. This implies that we don't have a single 'diffusion constant' for one species, but multiple (effective) diffusion constants referring to a number of species. We will come back to the 'spatial contingency' of these diffusion constants (see Section 4.4 below).

Can we make use of some general biological principles like the relation between body size and litter size (number of offspring) (e.g., the Janis and Carrano hypothesis, for terrestrial mammals) [27,28]? Or, between size and dispersive speed?

Given the proportionality between the size of an animal (A) and its velocity (L/t), as previously stated [14], the characteristic time dimension (τ) in terms of the species-specific parameters α, β and the physical time (t), may be approximated by:

$$\tau(A) \sim \frac{\alpha L^{\beta}}{\frac{L}{t}} = \alpha L^{\beta-1} t.$$

The combination of several of these relationships, in theory, might explain why only a limit number of large predators may cut down or limit the exponential growth of populations of smaller (and also some of the larger) herbivorous species. Obviously, we have to account for a considerably larger degree of complexity to analyze proper interspecific relations in multi-trophic ecosystems [24].

There is (only) a slight similarity of the conductive flow equation shown at the top of this paragraph, and the following equation, derived by Metz and Diekmann [29], describing the spread of an epidemic in an age-structured populations, with d_i and d_m the diffusion constants for the immature, resp. mature individuals of a species (see also [11]):

$$\frac{\partial u_m}{\partial t} = d_m \frac{\partial^2 u_m}{\partial x^2} + \alpha e^{-\gamma\tau} \int_{-\infty}^{\infty} \frac{1}{\sqrt{4\pi d_i \tau}} e^{\frac{-(x-y)^2}{4 d_i \tau}} u_m(y, t-\tau) dy - \beta u_m^2.$$

Moreover, Metz and Diekmann had found that, in the case of an 'immobile immature phase', the d_i would become zero and a Dirac delta function (δ) was found [29]:

$$\frac{1}{\sqrt{4\pi d_i \tau}} e^{\frac{-(x-y)^2}{4 d_i \tau}} = \delta(x-y),$$

implying that:

$$\int_{-\infty}^{\infty} \frac{1}{\sqrt{4\pi d_i \tau}} e^{\frac{-(x-y)^2}{4 d_i \tau}} u_m(y, t-\tau) dy = \int_{-\infty}^{\infty} \delta(x-y) u_m(y, t-\tau) dy = u_m(x, t-\tau).$$

Or, the mathematical expressions show a better correspondence than the initial case descriptions.

4. Parallel and anti-parallel developments

4.1. The single vs. multi-species problem in biodiversity

Starting from the ODE's for a three-species wavefront model for the spread of an epidemic, according to Murray [30], a general solution shows the product of a periodic and exponential function, such as:

$$s(x,t) = s_0 + A\cos[\omega(t + x/v) + \psi]\exp[-\lambda(t + x/v)],$$

for a single species (s) at some time (t) and distance (x) from the source of the epidemic.

When considering the similarities in distribution and propagation of the abundance patterns (and fluctuations) of different species in a geographical area, theoretically, a number of k species may be represented by a set of $n \times n$ matrices (with only real positive values A^1_{ij}, A^2_{ij}, … A^k_{ij}, i.e., the abundance patterns at a given moment t_0 for the species 1 to k).

Comparison of species that are evolving in parallel vs. anti-parallel evolving patterns, results from calculating the min, resp. max of the following operation:

$$D_{\max} = \sup_{1\to k} \{(|A^1_{ij} - A^2_{ij}|)/A^1_{ij}\} \text{ for all } k \text{ and } i \neq j \text{ (*)}.$$

(* We use capitals for the A^k matrices of k different species and lower-case symbols for the individual i,j-entries of the $n \times n$ matrices.)

The above operation however doesn't coincide with multiplying $|A^1 - A^2|$ with A^{-1} (or the inverse matrix of A^1), not only because not all $n \times n$ matrices are invertible [31], but in fact, the operation represents a different re-scaling of the original data set than is commonly used. Here, we may benefit from a paradigm developed by A. M. Turing's (1912–1954) in the previous century, that we'd like to introduce and propose a novel ecological application (see Section 4.2 below).

4.2. Turing's flow matrix paradigm

Turing's posthumously published description of so-called 'flow matrices' was originally related to the problem of continuously changing phyllotaxis and the use of 'inverse lattice'-concept [32]. Turing's own definition of 'flow matrices' was formulated as follows [32]:

If a lattice is changing, the manner of its change may be described by some matrix description $A(t_0)$ of the lattice at some time t_0, together with the product $(A(t))^{-1}A'(t)$ at other times, the dash here representing differentiation. This product will be called the 'flow matrix'. It is independent of the matrix description chosen, for if $B(t)$ is another matrix description there is an improper unimodular matrix L such that $B(t) = LA(t)$, and if $A(t)$ and $B(t)$ are continuous, L must be constant. But then:

$$(B(t))^{-1}B'(t) = (LA(t))^{-1}LA'(t) = (A(t))^{-1}A'(t)$$

Although the notion of lattices, according to Turing "is no longer appropriate when discussing the origin of the phyllotactic pattern", it is "nevertheless appropriate to describe functions on the surface of a cylinder by a Fourier analysis of some kind" [32]. He also noticed that the description of these phyllotactic patterns is similar to the description of electron density in a crystal [32], as was first observed by the brothers Louis et Auguste Bravais in 1837 [33]. According to Turing, the theory of flow matrices is derived from the analysis of Joseph Fourier (1768–1830) for functions derived on a cylinder: the appropriate kind of Fourier analysis for such functions is of the general form of a Fourier series in one variable and a Fourier integral in the other (see also Appendix A of [34]), as shown in the formula of [32]:

$$f(x,y) = \sum_{m=-\infty}^{\infty} \int_{-\infty}^{\infty} F_m\,(v) e^{(\frac{imx}{P}+ivy)} dy,$$

although the function $F_m(\upsilon)$ in general will not be easily represented (in a diagram), Turing cautions, because of its complex nature.

Using the matrix description in helical coordinates [32], Turing derives the following notation for the flow matrix, e.g., of a phyllotactic pattern in developing plant buds.

$$F = \begin{pmatrix} F_{11} & F_{12} \\ F_{21} & F_{22} \end{pmatrix} = \begin{pmatrix} \frac{d \log \rho}{dt} & 0 \\ \frac{\rho}{\eta} \cdot \frac{d\alpha}{dt} & \frac{d \log \eta}{dt} \end{pmatrix}.$$

For a lattice which changes continuously with time from $A(t_1)$ to $A(t_2)$, the ratio $(A(t_1))^{-1}A(t_2)$ is called the "finite flow matrix" for the period t_1 to t_2. Further, Turing suggests that if a flow matrix is independent of time, the corresponding finite flow may be expressed as the exponential of the product of the flow and the time for which it acts [32]. An example of a relevant case of an exponential of matrices is given by:

$$\exp\begin{pmatrix} 0 & \theta \\ -\theta & 0 \end{pmatrix} = \begin{pmatrix} \cos\theta & \sin\theta \\ -\sin\theta & \cos\theta \end{pmatrix},$$

following from the following calculation rules for exponentials of matrices, namely

$$\exp(A) = I + A + A^2/2 + \ldots + A^n/n!$$

(for A being a rectangular matrix), which in the example given above indeed yields the given matrix [32]:

$$\exp\begin{pmatrix} 0 & \theta \\ -\theta & 0 \end{pmatrix} = \begin{pmatrix} 1 & 0 \\ 0 & 1 \end{pmatrix} + \begin{pmatrix} 0 & \theta \\ -\theta & 0 \end{pmatrix} - \begin{pmatrix} \theta^2 & 0 \\ 0 & \theta^2 \end{pmatrix} + \cdots = \begin{pmatrix} \cos\theta & \sin\theta \\ -\sin\theta & \cos\theta \end{pmatrix},$$

since:

$$\begin{pmatrix} 0 & \theta \\ -\theta & 0 \end{pmatrix}^2 = \begin{pmatrix} \theta^2 & 0 \\ 0 & \theta^2 \end{pmatrix} \cdot (-1)^{\frac{2}{2}}.$$

The latter exponential of matrices is analogous to the relationship between the Taylor (1685–1731) series expansions of exponential and geometric functions (also known as Euler's formula) (1707–1783), or:

$$\exp(ix) = \cos x + i \sin x.$$

The matrix chosen by Turing [32] (see above) also fulfills the criterion for invertibility, namely $A \cdot A^{-1} = I$ which is shown below in the case of the 2 × 2 matrix. (Note that the determinant of the matrix above equals 1, since for any θ, we have $\cos^2 \theta + \sin^2 \theta = 1$. This is especially helpful, when calculating the inverse matrix A^{-1} from A). And, therefore:

$$\begin{pmatrix} \cos\theta & \sin\theta \\ -\sin\theta & \cos\theta \end{pmatrix} \cdot \begin{pmatrix} \cos\theta & -\sin\theta \\ \sin\theta & \cos\theta \end{pmatrix} = \begin{pmatrix} 1 & 0 \\ 0 & 1 \end{pmatrix} = I_2^2.$$

The latter matrix multiplication—corresponding with a (anti-)clockwise rotation with angle θ—is reminiscent of a special class of invertible matrices, known as the Pauli (1900–1958) spin matrices used in physics [31], such as:

$$\sigma_2^2 = \begin{pmatrix} 0 & -i \\ i & 0 \end{pmatrix} \cdot \begin{pmatrix} 0 & -i \\ i & 0 \end{pmatrix} = I_2^2.$$

Turing [32] applied the (finite) flow matrices for various ends, related to the growth of fixed patterns in plant morphogenesis, and suggested it could also become useful to describe the unrolling (literally by unfolding a cylindrical pattern) of epidemics in a planar configuration [35]. In principle, this approach would also allow to describe a flow pattern of changing interacting species in time, but, so far, this remains a theoretical possibility. We here suggest the combination of the flow matrices with Laplace transform as a new mathematical application.

In continuation of the use of Laplace transforms to the description of the border phenomena [14], we forward the following Laplace transforms *I* and *J*, respectively of the cosine and sine functions of (qt) with $q \neq 0$.

$$I = L\{\cos qt\},$$

$$J = L\{\sin qt\}.$$

Again, using Euler's formula and solving the defined integral, we obtain the following results for *I* and *J*, assuming $s > 0$ [36]:

$$I + iJ = \int_0^\infty e^{-st} \cos qt\, dt + i \int_0^\infty e^{-st} \sin qt\, dt,$$

$$I + iJ = \int_0^\infty e^{-st} e^{iqt} dt = \left[\frac{e^{-(s-iq)t}}{(s-iq)}\right]_0^\infty = 0 + \frac{1}{(s-iq)} = \frac{(s+iq)}{(s^2+q^2)},$$

$$I = L\{\cos qt\} = \frac{s}{(s^2+q^2)},$$

$$J = L\{\sin qt\} = \frac{q}{(s^2+q^2)}.$$

Taking the Laplace transform of the matrix $F(t)$, for a fixed angle $\theta = qt$, we then obtain:

$$L\{F(t)\} = \int_0^\infty e^{-st} F(t) dt = \int_0^\infty e^{-st} \begin{pmatrix} \cos\theta & \sin\theta \\ -\sin\theta & \cos\theta \end{pmatrix} dt,$$

$$L\{F(t)\} = \begin{pmatrix} \frac{s}{(s^2+q^2)} & \frac{q}{(s^2+q^2)} \\ \frac{-q}{(s^2+q^2)} & \frac{s}{(s^2+q^2)} \end{pmatrix} = \frac{1}{(s^2+q^2)} \begin{pmatrix} s & q \\ -q & s \end{pmatrix}.$$

The challenge to be solved remains, however, the combination of multiple overlapping patterns corresponding to a real dynamical ecosystem, with multiple co-habiting species [14]. In an anthropogenic, agriculturally controlled landscape, we may expect some seasonal periodicity with synchronized growth and abundance patterns, due to seeding, growing, mowing or grazing activities. Moreover, planned human interference may in part control the succession of a series of species with interrelated characteristic timing dimensions. Mathematically, we may write $\theta = qt = 2\pi k_i t/\omega$, with k_i a species-specific constant and ω the characteristic angular velocity. However, many more unpredicted interactions with other species than the controlled ones, may cause deviations from the wanted or predicted patterns.

4.3. Growth and recycling in the border interface

In order to characterize the ecological border interface in mathematical terms, we start from the logistic growth function $y(t)$ in terms of the carrying capacity (L) and a logistic growth rate k, $k > 0$, expressing the steepness of the curve. The logistic growth function, originally introduced by Verhulst (1804–1849) [37] as an adaptation of the exponential growth model of Quetelet (1796–1874), is given by:

$$y(t) = \frac{L}{1+e^{-kt}},$$

$$\frac{L}{y(t)} - 1 = e^{-kt}.$$

Rewriting $L - y(t) = G(t)$ for the (maximum) growth potential (or the 'available' carrying capacity), and with $y(t) = g(t)$, the following logistic growth ratio is expressed as a Taylor series:

$$\frac{G(t)}{g(t)} = e^{-kt} = 1 + \frac{(-kt)}{1!} + \frac{(-kt)^2}{2!} + \cdots \frac{(-kt)^n}{n!} = \sum_{n=0}^{n} \frac{(-kt)^n}{n!}.$$

The growth rate of the border interface, however, not only refers to the growth of plant species, e.g., trees defining a fractal border between forest and grassland [38]. It is a complex process, involving both linear growth ($p_i(t)$), as well as ramifications or branching points ($q_i(t)$) [8], and a term for destruction, decay or recycling ($s_i(t)$) of the previously grown material. In terms of the 'worm paths', this process can also mean the 'predator eating its way' in an existing population of prey species, or primary producers (see Section 4.4 below).

$$k_i(t) = p_i(t) + q_i(t) - s_i(t),$$

$$s_i(t) \cong \sigma \cos \eta t.$$

The complexity of this active, fractal border-generating process, becoming a true interface between different habitats, is also analogous to the connectivity distribution derived by Albert and Barabasi, as mentioned before [20]. Moreover, the successive steps in this fractal-generating process allow for an iterative procedure. In non-degenerative conditions, implicating that $p_i(t) + q_i(t) > s_i(t)$, the growth potential in the i-th phase, depends on the resources made available in the preceding phase, or:

$$\frac{dG_i}{dt} = k \cdot e^{-kt} \int_0^t s_{i-1}(\tau) s_{i-1}(t-\tau) d\tau.$$

Solving the above integral-differential equation, making use of the Laplace transform (as worked out in Section 4.2), the following (theoretical) result appears:

$$G_i(t) = \int_0^{\infty} e^{-kt} \left[\int_0^t s_{i-1}(\tau) s_{i-1}(t-\tau) d\tau \right] dt$$

$$= \int_0^{\infty} e^{-kt} \left[\int_0^t \sigma_{i-1} (\cos \eta\tau) \cos \eta\, (t-\tau) d\tau \right] dt$$

$$= L\{F_1(s_{i-1}(\tau)) F_2 s_{i-1}(t-\tau)\}.$$

Finally, when the border interface grows into a fractal-like network with extensions, ramifications and holes in it, then also the availability of ecological niches rises, and consequently, the potential for animal biodiversity (and of other life forms related to these habitats). Relating the theoretical, optimal biodiversity potential ($B_{opt}(t)$) to the similarity (or topological) dimension (D) [39], with σ_i the characteristic amplitude for cyclic growth and replacement at the lowest (microscopic) scale and the time-averaged estimates of p, q and s at the i-th iteration level, we obtain a new estimate for the similarity dimension D:

$$D = \lim_{\sigma_i \to 0} \frac{\ln\left(B_{opt}(t)\right)}{\ln(\sigma_i)} \cong \frac{-(\widehat{p_i} + \widehat{q_i} - \widehat{s_i})}{\ln(\sigma_i)}.$$

4.4. Antagonism, neutral interactions and morphic resonance

Before discussing the biological significance of the mathematical features described above, we'd first dwell into a little historical and philosophical discourse. In the eighties of previous century, the British biologist and philosopher Rupert Sheldrake (1942, Newark-on-Trent, England) proposed a physical hypothesis in order to explain so-called diachronic causal relationships (in biology), designated as 'formative causation' [40]. These 'formative causation' relationships, according to Sheldrake, might explain the interaction between entities that are separated in time and place, and thus do not need a direct, localized transfer of energy or momentum. Sheldrake proposed the term 'morphic resonance', in analogy with the resonance notion in physics (in acoustics, in subatomic physics and nuclear magnetic resonance, et cetera), but with also many examples in the field of biology [40]. Sheldrake's notion of 'morphic resonance' however was met with skepticism and fierce criticism, his work being denounced as pseudo-science, probably due to his affiliation with parapsychology and other disciplines outside of mainstream science [41]. The latter criticism apparently reverberated long after the publication of Sheldrake's monography [40], which in itself formed an interesting illustration of the 'formative causation' principle (even before the rise of Internet critiques and social media), with no direct physical interaction between the physicists blaming Sheldrake for his digressions [41,42].

Although resonance is a well-known phenomenon in the physics of oscillations, the transfer of this notion to the field of morphogenesis and morphogenetic mechanisms, indeed is a tedious and cumbersome piece of work. Sheldrake remarked that the size of morphogenetic fields is crucial, although not much specific information on the relation between these fields and their size was given (except for the general quadratic and cubic relationships between size of a body and energy exchange, as well as the characteristics of field polarity and stability of a morphogenesis, which are suggested to be already present at the molecular level) [40]. And, indeed, apart from the multi-species models where food competition or direct energy transfer occurs through the eating of one species by another, the interaction of different species without a localized transfer of energy or momentum is hard to explain in conventional physics terms. Moreover, although the interaction through visual, auditive or olfactory signaling could presumably be reduced to light, acoustic or chemical signaling, it is not the pattern of photons, the typical sound or noise, or chemical substances, that directly exchanges energy with the recipient animal. Otherwise, 'fear' of being attacked by a predator, might make the energy available for the animal to flee. So, in the end, awareness or fear may cause animals to avoid interaction (also with humans see Section 5. Historical contingencies and species-specific deviations) and form segregated distribution patterns. However, in rare occasions, predators and prey are enclosed in an area where it is almost impossible for the prey to completely escape sight from the predators: such is seen in the Ngorongoro Crater (Arusha region, Tanzania), where Lions, Hyenas, Gazelles and many antelope species and other predators live at close distance from one another. In the case of plants that are signaling through chemical substances with each other, and doing so providing a plant defense system against their assailants, the chemical mechanism involved and energy exchange are not less complicated.

Finally, it is the mathematical description of patterns of interaction that may mirror the patterns seen in (natural) wildlife, without 'direct physical interaction' with the biological species or individuals, giving again an illustration of what Sheldrake called a "dualism between mathematics and physical reality" [40], in some 'metaphorical' way mimicking the wave-particle duality of physical entities [43]. However, in Sheldrake's metaphorical usage of this duality, no confining element like the Planck constant is present, referring to the pioneering physicist Max Planck (1858–1947), and therefore, Sheldrake's universal duality between mathematics and reality offers no starting point for direct analysis. As a result, in order to apply for instance reaction-diffusion theory to biological processes, and to ecological dispersion phenomena in particular, the spatio-temporal contingency of these systems forms an important conceptual link [44].

The antagonism or neutrality of patterns of interaction between different species, moreover, follows from direct observation of the ecological phenomena. The same holds for the susceptibility to infection with viruses, parasites and other zoonotic epidemics.

However, another analogy may find some popular imitation, such as the computer-generated quasi-fractal replications of natural phenomena with the name Worm Paths [45]. Obviously, not much imagination is needed to represent the areal distribution pattern of a certain (number) of species in a two or three-dimensional graphic. The technique for drawing such patterns was proposed already long ago, namely by Frank C. Odds (1945, Devon, UK), John H. Conway (1937–2020) and Mike Patterson (1942, UK), who invented the concepts and rules for generating patterns by so-called 'spirolaterals' [46,47]. Also, when considering the border interface between two biotopes, characteristic pioneering species of either side may 'eat their way' in the adjacent biotope, like the 'prehistoric worms' did in M. Beeler's memorandum of 1973 [45,47] (see also Section 4.3). On top of these fractal-generating activities of pioneers (e.g., spruce seedlings adjacent to a spruce forest, or grasses from an adjacent grassland, or saprophytic fungi feeding on the previous), the patterns thus generated may become a stepping-stone access for other species. So, no longer the geometric, regular lattice of squares, triangles or hexagons, but a so-called stochastic fractal pattern forms the starting point for a further fractal-like repatterning of the entire ecosystem.

5. Historical contingencies and species-specific deviations

In the following paragraph, an example is given from observations in the Netherlands, the so-called Raven-Wolf-Deer alliance in forest ecology. It is a well-known example (at least among foresters and wildlife managers) that Northern Raven (*Corvus corax*) follow the dispersion of Wolves (*Canis lupus*) in the Northern Hemisphere, because the two species have mutual benefits in either finding, killing and opening (by wolves) of the hunted prey (especially deer and wild hog). Therefore, it shouldn't be surprising that after the disappearance since 1924 from the Netherlands [48] and from North-West Europe (with the exception of Scotland and Ireland, as well as a few rare observations), the Northern Raven convincingly re-appeared in the mid-

2010s in the Netherlands [49]. Not only a remarkable increase of sightings but also an exponential increase in breeding numbers of the Northern Raven was reported [49]. Also the Wolf disappeared from the Netherlands (already since 1869) [50], and, although the first-found specimen was found to be the victim of a wildlife crime and probably didn't enter the Netherlands by itself [50], the species did return one year later in 2014 (news confirmed in a multitude of newspapers and local news media). The alleged East-European origin of the first wolf of 2013 was based on the examination of its DNA haplotype and of the ^{87}Sr/^{86}Sr isotopes retrieved from both the dead wolf and the beaver remains in its stomach [50]. So, the re-appearance of the Wolf in the Netherlands, occurred quite simultaneously with the return of the Northern Ravens (own observations and [49]).

Less well-known is what caused the settlement of territorial wolves and the rapid increase of wolve pack numbers in the central region of the Netherlands (known as the Veluwe area) since 2018, whereas in the remaining parts of the Netherlands, only solitary or small groups of at most a couple of wolves where found roaming the area. According to the Dutch data authority, the Centraal Planbureau voor de Leefomgeving (PBL also known as Bij12), the distribution of wolves since 2014 corresponds with the distribution of large forested areas in scarcely populated regions, and therefore, with infrequent encounters between humans and wolves [51] (see **Figure 1**).

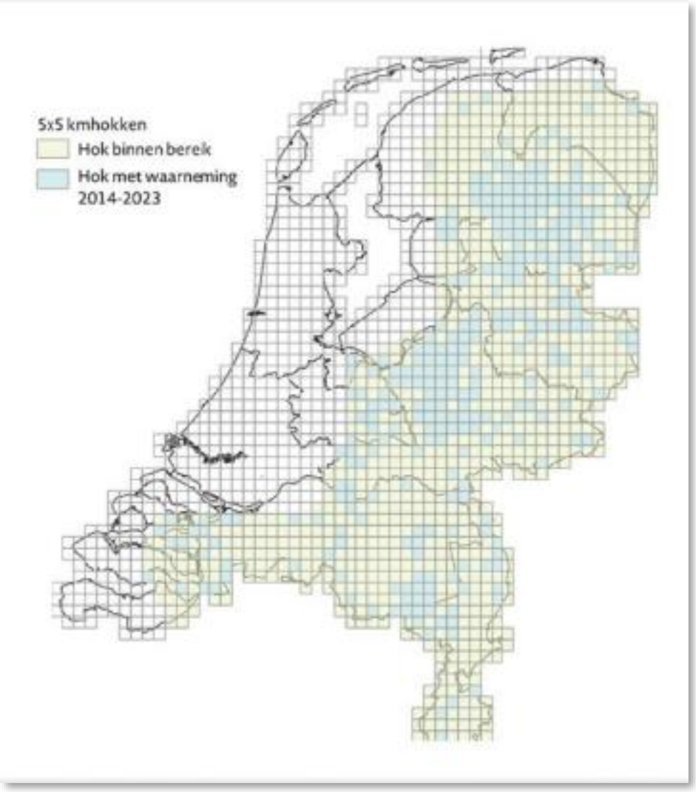

Figure 1. Geographical distribution of Wolves (*Canis lupus*) in the Netherlands in the period 2014–2023, based on Dutch national records of confirmed Wolf sightings and traces (5 × 5 km^2 squares; blue areas represent confirmed cases) [51].

The central region (Veluwe) of the Wolf distribution area, appears to be also the dominant geographical region for the distribution of Red Deer (*Cervus elaphus*)

(**Figure 2**), as well as for the distribution of the Wild Hogs (*Sus scrofa*), with the exception of the population at the Natural Park De Meinweg at the border between the province of Limburg and Germany (**Figure 3**). These regions correspond with areas where, for more than a century, large populations of Red Deer and Wild Hogs lived in (semi-) fenced areas. The origin of these fenced territories dates back to 1895, when the building of fenced preserves started in the forests of Hoog-Soeren and Wiessel, and until 1952, new forest areas became fenced at Vierhouten, the High Veluwe and in the Dutch Crown domains [52]. During the preceding centuries, nobilities and especially the Dutch royal domains, had played a prominent role in the preserving of game animals, although the Red Deer population gradually declined from pre-historical times until the eighteenth century, mostly due to deforestation and land cultivation [53]. Deforestation forced the deer to flee the river delta and to withdraw into the dunes of the provinces North- and South-Holland, where they also disappeared around 1750 [53]. Following the re-introduction and fence-closing activities, as well as the gradual enlargement of the forest occupied territory, the population of Red Deer increased in the twentieth century (after another low during the war years [1940–1945]), but mostly remained confined to the Veluwe region. The smaller Roe Deer (*Capreolus capreolus*), however, already re-populated the Dutch forests at large, starting from 1855 [52]. In the recent decades, in the dunes of North-Holland, also a stable population of Fallow Deer (*Dama dama*) had settled, causing a lot of nuisances to the local human residents.

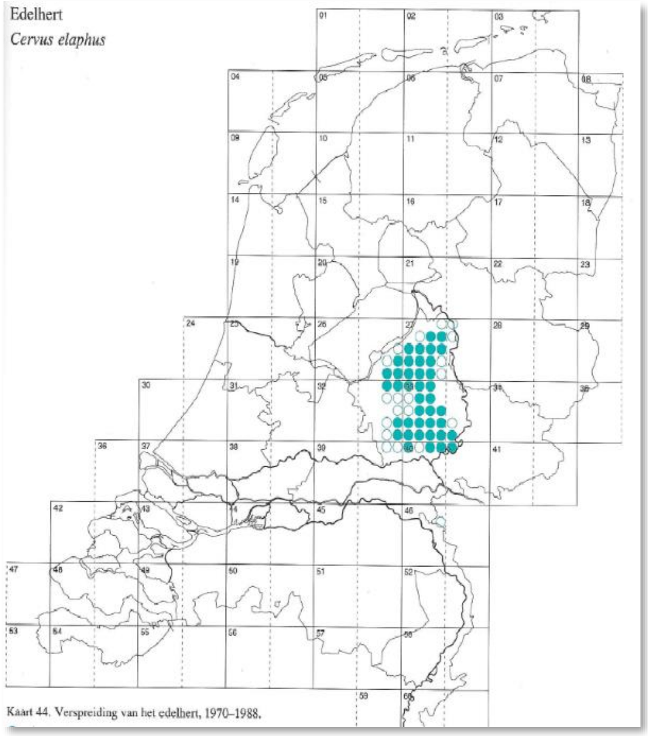

Kaart 44. Verspreiding van het edelhert, 1970–1988.

Figure 2. Geographical distribution of Red Deer (*Cervus elaphus*) in The Netherlands, from 1970–1988.

Note: Data obtained by Dutch national record collection and collected records of volunteer data. Translation of the legend in Dutch: Filled circles represent persistent populations (also to the present), open circles represent wandering specimen, or so-called ‘wisselwild’ [52].

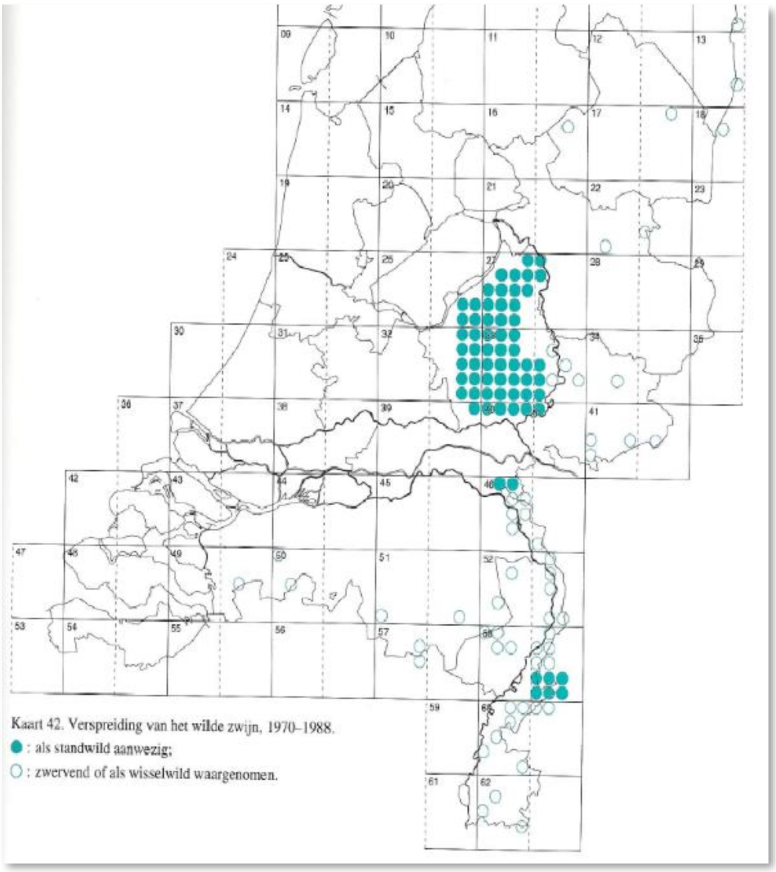

Figure 3. Wild Hog (*Sus scrofa*) in The Netherlands, from 1970–1988.

Note: Data obtained by Dutch national record collection and collected records of volunteer data. Translation of the legend in Dutch: Filled circles represent persistent populations (also to the present), open circles represent wandering specimen, or so-called 'wisselwild' [52].

So, although the availability of prey species (deer, wild hog, beaver, etc.) for a top predator like the European Wolf has largely exceeded the fenced preserves of the Veluwe, it appeared that only in the latter region, the social animals were inclined to form territorial, socially-hunting packs. This is also known from wolves in other continents, like in the North-American Yellowstone National Park [54]. Recent studies in Yellowstone reported hunting packs with an average pack size of 10 to 11 wolves, predominantly chasing Elk (Wapiti, *Cervus canadensis*), Bison (*Bison bison*), Mule Deer (*Odocoileus hemionus*) and other ungulates. In absence of the larger prey species, "solitary wolves in search of a territory or mate are usually very shy" [50], and are compelled to feed on smaller prey. Nonetheless, the recent winter low of the Roe Deer (*Capreolus capreolus*) population (2024–2025), allegedly following a Bluetongue epidemic spilled-back from domestic sheep to wild deer, may or may not be related to the much reported low in the Dutch wolf population at the end of 2024. For, almost 25% of the record of the wolf population in the Netherlands (approximately ca. 20 animals) were reported 'missing' (news from Dutch national data authority, reported in several local newspapers). This reported low, however, could also be the result of illegal practices (see also [50]), or a temporal fluctuation resulting from unknown causes, that aren't explained in any of the models. The enormous distances traversed by wandering wolves, often exceeding hundreds of kilometers daily [50], may equally well be explained by the wolf's need to find new foraging areas.

The example depicted above not only illustrates the inherent difficulties of nature preservation and wildlife management, it is also an illustration of the difficulties of applying mathematical models to complex biological issues like ecosystems. Moreover, the constant interference of anthropogenic factors with natural ecosystems, such as in conservation, (de)forestation or agriculture issues, points to the trivial conclusion that, especially in the forgotten lacunae and border zones of human controlled land use, nature finds its uncontrolled escapes and opportunities for unpredicted adaptation. But, on the other hand, landsliding and apocalyptic catastrophes that spare no living being (like volcanic eruptions, tsunamis, and sometimes also a pandemic has a similar outcome), obviously have an all-enveloping effect and global fall-out. Recent human pandemics (related to the *Coronavirus* and related species) and zoonotic epidemics (e.g., *Ebola*-epidemic) have shown the global impact and spreading speed of the viruses and other pathogenic organisms. According to classical epidemiological studies, the so-called hair-trigger effect would predict an all-encompassing effect, provided a threshold condition is surpassed [20,29]. However, in case of the COVID-19 pandemic, factors related to the regulation of global human transport and compliance to protective measures were considered of primary importance to contain the pandemic [11].

In matters of ecosystem preservation, catastrophes appear as shock waves comparable to the ripples of waves reaching the river banks after a river boat passing. In the example of the Northern Raven accompanying the territorial expansion of the European Wolf (see above), the association is fast, almost immediate, only hampered by the time needed for finding suitable breeding locations. The idiosyncratic nature of these correlations was also mentioned by Hengeveld [21,22]. Other examples of ripples in the occupation of habitats, are for instance witnessed in many bird species, such as the Greenfinch (*Carduelis chloris*) (see also Section 1. Introduction). The latter species showed a sudden drop in numbers in 2006 in the UK, and a few years later (2009) also in the Netherlands. The reported cause was an infectious disease, caused by an infection with a Protozoan parasite (*Trichomonas gallinae*), which is common in doves and other bird species [55,56]. Apparently, the spread of the epidemic is facilitated by the widespread use of bird-tables for feeding, where doves, greenfinches and *Trichomonas sp.* meet and the infection is proliferated. A sudden drop, however, may be followed by a sudden recovery of a population, as mentioned above. The idiosyncratic nature of these interactions between species, follows from the characteristic time frame of the interspecies contact effects and reactive processes. Some species may indeed quickly recover, whereas other species are doomed to disappear after even a minor dip in abundance numbers.

In other than the common Finch species of the family of *Fringillidae*, such as in the Brambling (*Fringilla montifringilla*), the Linnet (*Carduelis cannabina*), and to some degree also the Siskin (*Carduelis spinus*), a more gregarious, wandering behavior is displayed in (large and mixed) forested areas, especially during the European winter period [48]. These species also show less opportunistic adherence to human settlements. It follows that the occurrence of the latter species may be less predictable for human observation (e.g., observable at the man-made bird-tables). The fortuitous encounters with them mostly follow the pattern of succession of the seasons and the eventual location of the animal's food sources in the forests.

6. Conclusion

In the present paper, the physical world of biological ecosystems is confronted with the realm of mathematical modeling. Two important characteristics stand out, namely the seemingly coincidental appearance of disturbances (called idiosyncrasies) and the persistent interference of human activities on the natural ecosystems (also called the anthropogenic footprint or the topology of the Anthropocene) [57]. So, when applying the mathematical tools to the ecosystems studied, such as reaction-diffusion and time-fractional diffusion modeling [25,26,32], Laplace transforms [14], (finite) flow matrices [32], Verhulst (logistic) dynamics [37], the idealized mathematical models show both striking similarities and unpredicted, species-specific deviations [21,22]. Moreover, in the cases of the often problematic correlations between big game and large predator species, also the historical origins (and human role in these historic influences) are important to understand the present ecosystem dynamics, in addition to the actual dynamics in the area (see Section 5. Historical contingencies and species-specific deviations).

The role in biodiversity resilience of the less controlled lacunae and border zones between human-controlled areas forms an interesting paradigm for further research, provided the human interference factor can be ruled out, e.g., by taking away fences and cattle-grids that block the spread of ungulates but not the spread of big predators. The mathematical approach presented in the present study, using a combination of reaction-diffusion, flow matrices and Verhulst logistic growth dynamics, therefore may offer a compelling framework for mathematical modeling of actual ecosystems. Finally, it remains a challenge to improve the modeling tools in order to prevent further deterioration of the global biosphere in the context of a changing climate.

Conflict of interest: The author declares no conflict of interest.

References

1. Hallmann CA, Sorg M, Jongejans E, et al. More than 75 percent decline over 27 years in total flying insect biomass in protected areas. PLOS ONE. 2017; 12(10): e0185809. doi: 10.1371/journal.pone.0185809
2. Piatt JF, Parrish JK, Renner HM, et al. Extreme mortality and reproductive failure of common murres resulting from the northeast Pacific marine heatwave of 2014–2016. PLOS ONE. 2020; 15(1): e0226087. doi: 10.1371/journal.pone.0226087
3. Weston P. 'The scale is hard to grasp': Avian flu wreaks devastation on seabirds. Earth Island Journal. 2022.
4. Allen AR, Skuce RA, Byrne AW. Bovine tuberculosis in Britain and Ireland—A perfect storm? The confluence of potential ecological and epidemiological impediments to controlling a chronic infectious disease. Frontiers in Veterinary Science. 2018; 5. doi: 10.3389/fvets.2018.00109
5. Animal & Plant Health Agency (Department for Environment, Food & Rural Affairs). Updated outbreak assessment for bluetongue virus in Europe (updated September 11, 2024). Available online: https://www.gov.uk/government/publications/bluetongue-virus-in-europe (accessed on 8 March 2025).
6. Freedman HI. Deterministic Mathematical Models in Population Ecology. New York: Marcel Dekker; 1980.
7. Addicott JF. Stability properties of 2-species models of mutualism: Simulation studies. Oecologia. 1981; 49(1): 42–49. doi: 10.1007/bf00376896
8. Rai B, Freedman HI, Addicott JF. Analysis of three species models of mutualism in predator-prey and competitive systems. Mathematical Biosciences. 1983; 65(1): 13–50. doi: 10.1016/0025-5564(83)90069-X

9. Krikorian N. The volterra model for three species predator-prey systems: Boundedness and stability. Journal of Mathematical Biology. 1979; 7(2): 117–132. doi: 10.1007/bf00276925
10. Hsu SB, Ruan S, Yang TH. Analysis of three species Lotka-Volterra food web models with omnivory. Journal of Mathematical Analysis and Applications. 2015; 426(2): 659–687. doi: 10.1016/j.jmaa.2015.01.035
11. Allaerts W. Stochastic reaction-diffusion modeling and epidemiology in a post-COVID-19 era. Austin Journal of Public Health and Epidemiology. 2021; 8(5): 1112.
12. Renshaw E. Stochastic effects in population models. In: McGlade J (editor). Advanced Ecological Theory: Principles and Applications. London: Blackwell Science; 1999. pp. 23–63.
13. Volterra V. Variations in the number of individuals in coexisting animal species (Italian). In: Animal Ecology. New York: McGraw Hill; 1926. pp. 409–448.
14. Allaerts W. Towards a time-integrated convolution of the fractal biodiversity interface: The relation between biodiversity and entropy re-examined. Advances in Earth Science. 2025; 6(3): 1–9. doi: 10.47485/2766-2624.1071
15. Allaerts W. Life as a dissipative structure. A metabletic exploration of public health research. Communication & Cognition. 2024; 57(1-2): 105–126. doi: 10.57028/c57-105-z1060
16. Law R. Theoretical aspects of community assembly. In: McGlade J (editor). Advanced Ecological Theory: Principles and Applications. London: Blackwell Science; 1999. pp. 143–171.
17. Golubitsky M, Stewart I. The symmetry perspective. From equilibrium to chaos in phase space and physical space. Basel, Boston, Berlin: Birkhäuser Verlag; 2002.
18. Lyapunov AM. The General Problem of the Stability of Motion (Russian) [PhD thesis]. Kharkov University; 1966.
19. Goh BS. Global Stability in Many-Species Systems. The American Naturalist. 1977; 111(977): 135–143. doi: 10.1086/283144
20. Allaerts W. Evaluating the connectivity, continuity and distance norm in mathematical models for community ecology, epidemiology and multicellular pathway prediction. Journal of Physics: Conference Series. 2019; 1391(1): 012119. doi: 10.1088/1742-6596/1391/1/012119
21. Hengeveld R. Von Uexküll's Umwelt Concept Revived. Acta Biotheoretica. 2024; 72(4). doi: 10.1007/s10441-024-09487-9
22. Hengeveld R. Dynamic Biogeography. Cambridge: Cambridge University Press; 1990.
23. Carslaw HS, Jaeger JC. Conduction of Heat in Solids. Oxford: Clarendon Press; 1959. p. 29.
24. Allaerts W. The unified neutral theory of biodiversity and biogeography revisited. Advances in Earth and Environmental Science. 2023; 4(2): 1–10.
25. Allaerts W, Wouters A, van der Massen D, et al. A diffusion-adsorption model for the computation of the amount of hormone around a secreting cell, detected by the Reverse Hemolytic Plaque Assay. Journal of Theoretical Biology. 1988; 131: 441–459.
26. Youssri YH, Atta AG. Petrov-Galerkin Lucas polynomials procedure for the time-fractional diffusion equation. Contemporary Mathematics. 2023; 4(2): 230–248. doi: 10.37256/cm.4220232420
27. Janis CM, Carrano M. Scaling of reproductive turnover in archosaurs and mammals: why are terrestrial mammals so rare? Annales Zoologici Fennici. 1992; 28: 201–216.
28. Werner J, Griebeler EM. Reproductive Biology and Its Impact on Body Size: Comparative Analysis of Mammalian, Avian and Dinosaurian Reproduction. PLoS ONE. 2011; 6(12): e28442. doi: 10.1371/journal.pone.0028442
29. Metz AAJ, Diekmann O. The Dynamics of Physiologically Structured Populations. New York: Springer Verlag; 1986.
30. Murray JD. Mathematical Biology. Berlin, Heidelberg: Springer Verlag; 1989.
31. Brinkmann HW, Klotz EA. Linear Algebra and Analytic Geometry. Addison-Wesley Educational Pub; 1971.
32. Turing AM. Morphogen theory of phyllotaxis. In: Saunders PT (editor). Collected Works of A.M. Turing. Part3. Morphogenesis. Amsterdam, London, New York: North-Holland (Elsevier Science Publishers BV); 1953. pp. 69–88.
33. Bravais L, Bravais A. Essay on the arrangement of curviserial leaves (French). Annales Science Naturelle Botanique. 1837; (2): 42,193.
34. Allaerts W. Fifty years after Alan M. Turing: An extraordinary theory of morphogenesis. Belgian Journal of Zoology. 2003; 133(1): 3–14.
35. Allaerts W. Turing's apple. Or the emergence of a modern myth (Dutch). bi-logical. 2008; 1(1): 10–25.
36. Williams J. Laplace transforms. Series: Problem Solvers. London: George Allen & Unwin Ltd; 1973.

37. Verhulst PF. Notice on the law that the population pursues in its increase (French). Correspondance Mathématique et Physique. 1838; 10: 113–121.
38. Allaerts W. On land use and biodiversity resilience: Hydrology, temperature regulation and the fractal nature of the woodland-grassland interface. Austin Environmental Sciences. 2023; 8(2). doi: 10.26420/austinenvironsci.2023.1097
39. Allaerts W. Estimating biodiversity and the fractal nature of ecosystems. International Journal of Bioinformatics and Computational Biology. 2020; 5(1): 15–24.
40. Sheldrake R. A new science of life: The hypothesis of formative causation. London: Blond and Briggs; 1981.
41. Maddox J. A book for burning? Nature. 1981; 293: 245–246. doi: 10.1038/293245b0
42. Kayzer W, Sacks O, Gould SJ, et al. A Wonderful Accident (Dutch). Amsterdam, Antwerpen: Uitgeverij Contact; 1995.
43. de Broglie LV. On the Theory of Quanta [PhD thesis]. Foundation of Louis de Broglie; 1924.
44. Allaerts W. Inquiry into the spatio-temporal contingency of cellular communication systems. Communication & Cognition. 1992; 25(4): 277–294.
45. Gardner M. Knotted Doughnuts and other Mathematical Entertainments. New York: W.H. Freeman and Company; 1986. pp. 205–221.
46. Odds FC. Spirolaterals. The Mathematics Teacher. 1973; 66(2): 121–124. doi: 10.5951/mt.66.2.0121
47. Beeler M. Paterson's Worm: Artificial Intelligence Memo No. 290. Cambridge, MA: Massachusetts Institute of Technology; 1973.
48. Peterson RT, Mountfort G, Hollom PAD. A field guide to the birds of Britain and Europe. In: Kist J, Van Oordt GJ (translation). Vogelgids. Amsterdam, Brussel: Elsevier; 1962.
49. SOVON. Northern Raven. Distribution and trends (Dutch) (data 1990–2025). Stichting Vogelonderzoek Nederland (SOVON). Available online: https://stats.sovon.nl/stats/soort/15720 (accessed on 21 January 2025).
50. Gravendeel B, de Groot A, Kik M, et al. The first wolf found in the Netherlands in 150 years was the victim of a wildlife crime. Lutra. 2013; 56(2): 93–109.
51. Bij12. Verspreiding Wolf in Nederland (Dutch). Available online: https://www.bij12.nl/onderwerp/wolf/verspreiding-wolf-in-nederland/ (accessed on 21 January 2025).
52. Broekhuizen S, Hoekstra B, van Laar V, et al. Atlas of the Dutch Mammals (Dutch). Schoorl: Uitgeverij Pirola; 1992. pp. 197–207.
53. Brouwer GA. (1949). Some historical details about the red deer in the Netherlands and a reflection on the Veluwe deer as a nature conservation object (Dutch). In: In het voetspoor van Thijsse: Een reeks bijdragen over veldbiologie, natuurbescherming en landschap. Wageningen: H. Veenman & Zonen; 1949. pp. 214–247.
54. National Park Service. Yellowstone wolf project 2023. Available online: https://www.nps.gov/yell/learn/nature/upload/2023-Wolf-Report-final_web.pdf (accessed on 21 January 2025).
55. British Trust for Ornithology (BTO). Garden Birdwatch: Trichomonosis. Available online: https://www.bto.org (accessed on 21 January 2025).
56. Dutch Wildlife Health Center. Trichomonas sp. infection in a Greenfinch. Available online: https://www.dwhc.nl (accessed on 21 January 2025).
57. Morton T. Hyperobjects: Philosophy and Ecology After the End of the World. Minneapolis: University of Minnesota Press; 2013.